HHS Public Access

Author manuscript

Biomaterials. Author manuscript; available in PMC 2015 July 01.

Published in final edited form as:

Biomaterials. 2014 July ; 35(21): 5425–5435. doi:10.1016/j.biomaterials.2014.03.026.

Elastin Based Cell-laden Injectable Hydrogels with Tunable Gelation, Mechanical and Biodegradation Properties

Ali Fathi, **Suzanne M. Mithieux**, **Hua Wei**, **Wojciech Chrzanowski**, **Peter Valtchev**, **Anthony S. Weiss**[+], and **Fariba Dehghani**[1,+]

[1]School of Chemical and Biomolecular Engineering, University of Sydney, Sydney, Australia

[2]School of Molecular Bioscience, University of Sydney, Australia

[3]Faculty of Pharmacy, University of Sydney, Sydney, Australia

[4]Charles Perkins Centre, University of Sydney, Sydney, Australia

[5]Bosch Institute, University of Sydney, Sydney, Australia

Abstract

Injectable hydrogels made from extracellular matrix proteins such as elastin show great promise for various biomedical applications. Use of cytotoxic reagents, fixed gelling behavior, and lack of mechanical strength in these hydrogels are the main associated drawbacks. The aim of this study was to develop highly cytocompatible and injectable elastin-based hydrogels with alterable gelation characteristics, favorable mechanical properties and structural stability for load bearing applications. A thermoresponsive copolymer, poly(N-isopropylacrylamide-*co*-polylactide-2-hydroxyethyl methacrylate-*co*-oligo(ethylene glycol)monomethyl ether methacrylate, was functionalized with succinimide ester groups by incorporating N-acryloxysuccinimide monomer. These ester groups were exploited to covalently bond this polymer, denoted as PNPHO, to different proteins with primary amine groups such as α-elastin in aqueous media. The incorporation of elastin through covalent bond formation with PNPHO promotes the structural stability, mechanical properties and live cell proliferation within the structure of hydrogels. Our results demonstrated that elastin-*co*-PNPHO solutions were injectable through fine gauge needles and converted to hydrogels *in situ* at 37 °C in the absence of any crosslinking reagent. By altering PNPHO content, the gelling time of these hydrogels can be finely tuned within the range of 2 to 15 min to ensure compatibility with surgical requirements. In addition, these hydrogels exhibited compression moduli in the range of 40 to 145 kPa, which are substantially higher than those of previously developed elastin-based hydrogels. These hydrogels were highly stable in the physiological environment with the evidence of 10 wt% mass loss in 30 days of incubation in a simulated environment. This class of hydrogels is *in vivo* bioabsorbable due to the gradual increase of the lower critical solution temperature of the copolymer to above 37 °C due to the cleavage of polylactide from the PNPHO copolymer. Moreover, our results demonstrated that more than 80% of cells encapsulated in these hydrogels remained viable, and the number of

[+]Corresponding Authors: Weiss, A.S, tony.weiss@sydney.edu.au, Fax: +61-293514726, Dehghani, F, fariba.dehghani@sydney.edu.au, Fax: +61-293512854.

encapsulated cells increased for at least 5 days. These unique properties mark elastin-*co*-PNHPO hydrogels as favorable candidates for a broad range of tissue engineering applications.

Keywords

Thermally responsive material; Elastin; Hydrogel; Injectable

1 Introduction

Injectable biopolymer hydrogels display great promise for *in vivo* tissue engineering due to their high water uptake capacity and mass transfer capabilities [2], host tissue adhesive properties [3,4], biological similarity to natural extracellular matrix [5], tunable physicochemical characteristics [6,7], potential for encapsulation of cells, drugs, or growth factors [8,9], and minimally invasive method of delivery [10]. The elastin based hydrogels exhibit great potential for *in vitro* regeneration of dermal [11,12], cartilage [13] and cardiovascular tissues [14,15]. Low mechanical strength and lack of control on the gelation behavior and the use of cytotoxic crosslinking reagents are the main associated drawbacks to most of the current elastin based injectable formulations [9].

Different thermoresponsive monomers and polypeptides were chemically copolymerized to develop injectable hydrogels with tunable mechanical strength and gelation properties. The characteristics of thermoresponsive copolymer based injectable systems are modulated by changing the chemical composition of the copolymer and thus can be finely tuned to address specific clinical requirements [6,7]. In addition, the gelation of these thermoresponsive systems is triggered by increasing the temperature above the lower critical solution temperature (LCST) of the copolymers. This thermosetting behavior eliminates the need for addition of crosslinking reagents.

Poly(N-isopropylacrylamide) (PNIPAAm) is a water soluble, FDA approved thermoresponsive monomer with the LCST (~ 32 °C) close to physiological temperature, which makes it a favorable material for biomedical applications. Bioresorbable PNIPAAm-based copolymers have been developed via the copolymerization of PNIPAAm with synthetic degradable macromonomers and peptide sequences [7,16–18]. Due to the simplicity of its synthetic process and high mechanical strength, 2-hydroxyethyl methacrylate (HEMA)based macromonomers such as polylactide/HEMA (PLA/HEMA) have been widely used as hydrophobic backbones in PNIPAAm based copolymers [19]. Fixed physicochemical properties, lack of cell motif sites [18], and a fast degradation rate, such as 100% mass loss within 7 days [7] are the main limiting factors in clinical applications of these thermoresponsive hydrogels. Injectable biomaterials with tunable and favorable characteristics, therefore, are of vital need to address different clinical requirements.

The aim of this study was to develop a new class of thermoresponsive and bioresorbable material for a broad range of biomedical applications. To achieve this, a hydrophilic segment (oligo (ethylene glycol) monomethyl and a protein reactive site (NAS) were incorporated to the molecular structure of PNIPAAm-*co*-PLA/HEMA to form a water

soluble copolymer. We anticipated that the formation of covalent bonds between the copolymer and proteins would promote the structural stability and mechanical properties of this class of hydrogels. α-elastin was selected as a model protein with a relatively high number of lysine groups to investigate this effect on the characteristics of the hydrogels. We also hypothesized that the physicochemical and gelation properties of the resulting hydrogel could be finely tuned by changing the composition of the copolymer. In this study, the effect of copolymer formulation on the characteristics of hydrogels was investigated to produce a panel of materials with a wide range of properties. To the best of our knowledge this is the first injectable hydrogels with a tunable gelation, mechanical and bioresorption properties that can be finely modified for a specific clinical application.

MATERIALS AND METHOD

1.1 Materials

D,L-lactide (LA), stannous 2-ethylhexanoate ($Sn(OCt)_2$), N-isopropylacrylamide (NIPAAm), 2-hydroxyethyl methacrylate (HEMA), 4, 4′-azobis (4-cyanovaleric Acid) (ACVA), N-acryloxysuccinimide (NAS), Bradford reagent, Dulbecco's Modified Eagle's Medium (DMEM) and Fetal Bovine Serum (FBS) were from Sigma and were used as received. PrestoBlue® cell viability reagent was purchased from Life Technologies. Oligo(ethylene glycol) monomethyl ether methacrylate (OEGMA, Mn = 475, Sigma) was purified by passing a solution in dichloromethane (1:1 volume ratio) through a basic alumina column to remove inhibitors prior to use. LA monomer was dried under vacuum at 40 °C for 24 hr prior to use. α-elastin, extracted from bovine ligament, was obtained from Elastin Products Company.

1.2 Synthesis of PLA/HEMA

PLA/HEMA macromonomer was synthesized by ring-opening polymerization of lactide with HEMA using $Sn(OCt)_2$ as catalyst [19]. Known amounts of LA and HEMA were mixed in a 250 ml three-neck flask at 110 °C under nitrogen atmosphere for 15 min. A mixture of 1 mol% of $Sn(OCt)_2$ (with respect to HEMA feed) in 1 ml anhydrous toluene was then added to the LA/HEMA solution. The resulting mixture was stirred at 300 rpm at 110 °C for 1 hr under nitrogen blanket. The mixture was then dissolved in 20 ml tetrahydrofuran and precipitated in 200 ml cold (~1 °C) distilled water. The unpurified precipitated PLA/HEMA was separated by centrifugation at 3000 rpm for 5 min and the supernatant discarded. Cold distilled water was then added to the precipitated PLA/HEMA and the centrifugation process repeated twice to remove unreacted monomers and byproducts. The precipitated PLA/HEMA was then dissolved in ethyl acetate. PLA/HEMA macromonomer was further purified by centrifugation at 6000 rpm for 5 min. The supernatant was then dried by absorbing the residues of water by adding $MgSO_4$ particles and incubating this suspension for 18 hr at 25 °C. The particles of $MgSO_4$ were then removed by vacuum filtration. The purified polymer solution in ethyl acetate was dried at 60 °C under reduced pressure using a rotary evaporator. The solvent residue (mainly ethyl acetate) was further removed under vacuum at 40 °C for 24 hr. The resulting PLA/HEMA formed a viscous liquid and thereafter was stored at 4 °C. The feed ratio of LA:HEMA was varied from 1.5:1 and 2.5:1 to obtain PLA/HEMA macromonomers with different lactate numbers. The

formation of PLA/HEMA macromonomer and the lactate number were verified using ^{1}HNMR (Varian, 400 MR).

1.3 Synthesis of Poly(NIPAAm-*co*-(PLA/HEMA)-*co*-OEGMA-*co*-NAS)

Poly(NIPAAm-*co*-(PLA/HEMA)-*co*-OEGMA-*co*-NAS) denoted as PNPHO was synthesized by free radical polymerization, using ACVA as an initiator. Known amounts of NIPAAm, NAS, PLA/HEMA, OEGMA, and ACVA (7.0×10^{-5} mol as an initiator) were dissolved in 13 ml anhydrous N,N′-dimethylformamide in a 25 ml round bottom, one-neck flask. The system was then deoxygenated by at least three freeze-pump-thaw cycles, using liquid nitrogen as the coolant. The reactor was then sealed and immersed in an oil bath. The polymerization was conducted at 70 °C for 24 hr under gentle stirring (300 rpm). The resulting polymeric solution was then cooled at room temperature for 1 hr and precipitated in 250 ml diethyl ether. The precipitate was collected by filtering the suspension, and was subsequently dried under vacuum for 6 hr. The product was further purified by dissolving the dried powder in tetrahydrofuran and precipitating it in diethyl ether. The final product, PNPHO copolymer, was dried under vacuum for at least 48 h. The PNPHO was characterized with Gel Permeation Chromatography (GPC), ^{1}HNMR, and gas-chromatography techniques. Subscripts in PNPHO correspond to PLA/HEMA mol%(lactate number)OEGMA mol%.

1.4 Chemical bonding of PNPHO with proteins

The presence of succinimide ester groups in the molecular structure of PNPHO polymer provided active sites to bond with lysine-containing proteins such as elastin. In each run, a solution of 30 mg/ml of elastin and 150 mg/ml of PNPHO in phosphate buffered saline (PBS; 10 mM Na phosphate, 150 mM NaCl, pH 7) was prepared and stirred for 6 hr at 4 °C to chemically bond elastin and PNPHO. The solution was then moved to 37 °C to form an elastin-*co*-PNPHO hydrogel. Attenuated total reflectance Fourier transform infrared (ATR-FTIR) spectroscopy was used to confirm the chemical bonding between elastin and PNPHO. ATR-FTIR spectra were collected at a resolution of 2 cm^{-1} and signal average of 32 scans in each interferogram over the range of 1800–1500 cm^{-1} using a Varian 660 IR FTIR spectrometer.

1.5 Rheological and mechanical properties of elastin-*co*-PNPHO hydrogels

The rheological behavior of elastin-*co*-PNPHO hydrogels was investigated at different temperatures. The temperature was increased from 10 °C to 37 °C at a rate of 0.3 °C/min using a Physica rheometer. Parallel plates with a diameter of 25 mm were used and a sample with the thickness of 0.5 mm was placed between these plates. The gelling temperatures of elastin-*co*-PNPHO hydrogels fabricated with different compositions of PNPHO were recorded at the crossover point of the dynamic storage (G′) and loss (G″) moduli. In addition, the rheological behavior of elastin-*co*-PNPHO solutions was studied at 37 °C to determine the gelling time of hydrogels at physiological conditions.

An Instron (Model 5543) was used for conducting Uniaxial compression tests in an unconfined state with a 100 N load cell according to a previously described procedure [20]. Prior to the test, the samples were equilibrated in PBS for 2 h at 37 °C. The compression

(mm) and load (N) were collected using Bluehill-3 software at a cross speed of 50 μm/s. The compressive modulus was obtained as the tangent slope of stress-strain curve in the linear region, between 10 % – 20 % strain level.

1.6 Elastin and PNPHO chemical bonding efficiency-Bradford assay

The conjugation capacity of different compositions of copolymers was assessed by evaluating the retention of elastin within the copolymer structure after 24 hr of incubation in Milli-Q water (MQW). In each analysis 200 mg elastin-*co*-PNPHO hydrogel was soaked in 5 ml washing media (MQW) and left at 37 °C for 24 hr. The elastin concentration in the washing media was determined by the Bradford dye-binding assay [21,22]. In each test, 5 μl of washing media was mixed with 195 μl Bradford reagent in a 96 well-plate and left at room temperature for 25 min. The solution's absorbance was then measured at 595 nm using a microplate reader (Biorad 680). A standard curve of elastin concentration-absorbance was generated from at least 6 elastin standard solutions with absorbance in the range of 0.4 to 0.5. The samples were either diluted or concentrated to achieve the absorbance reading in the linear region (0.4 to 0.5).

1.7 *In vitro* cytotoxicity assay of degradation products

The degradation products of PNPHO hydrogels were used to assess the cytotoxicity of this class of polymers. For this study, $PNPHO_{8(6)5}$ was used as a model. The subscript 8, 6, 5 corresponds to the molar ratio of PLA/HEMA, lactate number), and OEGMA mol%, respectively. In each run 150 mg $PNPHO_{8(6)5}$ was dissolved in 1 ml of PBS at 4 °C. The temperature was then increased to 37 °C to form a hydrogel. The PNPHO hydrogel was then submerged in 5 ml PBS at 37 °C for one month to degrade the construct completely. A 1:3 volume ratio mixture of the degradation solution and standard culture medium (DMEM, 10 % FBS, Anti-Anti) was used to culture human dermal fibroblasts (GM3348) for 4 days to study the cytocompatibility of the degradation products from PNPHO copolymer. The culture medium (400 μl) was not replaced but was supplemented with 40 μl FBS daily. At different time intervals, cell viability was measured using a MTT assay for mitochondrial activity. For this analysis, the culturing medium was removed from the wells, then 250 μl of fresh medium and 50 μl Cell Titer 96 Aqueous One Reagent (Promega) were added to each well, and the cells were incubated at 37 °C for 1 hr. The solution absorbance was measured at 480 nm and compared to the standard culture (culture media without the degradation product).

1.8 Cell encapsulation

Cell encapsulation efficiency of PNPHO hydrogels was assessed. For this study, 150 mg of $PNPHO_{8(6)5}$ were added to 1 ml of PBS and gently stirred at 4 °C for 6 hr to form $PNPHO_{8(6)5}$ hydrogel precursor solution. In addition, a solution of 30 mg/ml of elastin and 150 mg/ml of $PNPHO_{8(6)5}$ in PBS was prepared to form elastin-*co*-$PNPHO_{8(6)5}$ hydrogel solution. These two solutions (each 1000 μl) were mixed separately with 10 μl dermal fibroblasts cell suspension (5×10^4 cells) at room temperature. The solutions were then converted hydrogels (elastin-*co*-PNPHO and PNPHO) by placing them at 37 °C for 15 min. These cell laden hydrogels were placed in standard culture media at 37 °C and 5% CO_2 for

up to 5 days. At different time points, these thermoresponsive hydrogels were liquefied by placing them at 4 °C for nearly 2 hr to release the encapsulated cells. Live cells were stained by addition of 10 v% Prestoblue and the resulting suspensions (cell-hydrogel) were then subjected to flow cytometry analysis. Cell debris, live and dead cells were differentiated, based on their forward scatter (size) and staining in flow cytometry dot-plot. Based on size (forward scatter) and staining, the events (dots) were separated into three populations: debris (R1), total cells (R2) [determined with cell-laden hydrogel solution without Prestoblue staining], and live cells (R3) [determined with cell-laden hydrogel solution with Prestoblue staining]. A preliminary test was conducted to validate this method by counting the viable cells with flow cytometry and comparing this result with manual counting of cells using a hemocytometer and trypan blue exclusion. One way Analysis of Variance (ANOVA) showed that there was no significant ($p>0.05$) difference between the results acquired with these two techniques. Flow cytometry was, therefore, used to determine encapsulation efficiency and cell viability on day 0, and cell proliferation from day 1 to day 5.

2 Results and Discussion

2.1 Synthesis of poly(NIPAAm-*co*-PLA/HEMA-*co*-OEGMA-*co*-NAS)

PNPHO copolymer was synthesized by random polymerization of thermoresponsive (PNIPAAm), mechanically strong (PLA/HEMA), protein reactive (NAS) and hydrophilic (OEGMA) segments. This copolymer was synthesized by free radical polymerization using 4, 4′-azobis (4-cyanovaleric acid) as an initiator in dimethylformamide at 70 °C for 24 hr. The scheme of this reaction is shown in Figure 1-a. The composition of copolymer was altered by varying the lactate number (3 or 6) in PLA/HEMA, mol% of PLA/HEMA (6, 8 or 11) and mol % OEGMA (3, 5 or 8). For this purpose, prior to synthesis of PNPHO, PLA/HEMA macromonomers with different lactate numbers were synthesized. In this study, the copolymer is denoted as PNPHO and the subscript corresponds to PLA/HEMA mol% (lactate number) and OEGMA mol%. For example, $PNPHO_{8(6)3}$ is shorthand for copolymer synthesized with 8 mol% PLA/HEMA with lactate number of 6, and 3 mol% OEGMA.

PLA/HEMA was synthesized by ring-opening polymerization of lactide with the hydroxyl group of HEMA as initiator and $Sn(OCt)_2$ as catalyst [19]. The synthesis of PLA/HEMA macromonomer was confirmed using ^{1}HNMR spectra with evidence of proton peaks from both HEMA and lactyl (LA) species. The molar ratio of LA to HEMA in PLA/HEMA macromonomer was calculated from ^{1}HNMR spectra using the peak at 5.2 ppm for the methine in lactate, and double bond peaks at 5.7 ppm and 6.0 ppm in HEMA. This molar ratio was reported in the form of a lactate number. Two PLA/HEMA macromonomers with lactate numbers of 3 and 6 were synthesized using 1.5:1 and 2.5:1 molar ratio of LA to HEMA monomers, respectively.

The synthesis of PNPHO copolymer was confirmed with ^{1}HNMR spectra with evidence of proton peaks for all segments, as shown in Figure 1-b. Characteristic proton peaks were detected for NIPAAm (a and b), NAS (e), PLA/HEMA (f, h, k), and OEGMA (m and n). The final molar concentrations of each segment in the copolymer were calculated based on the integration of peaks that are labeled in Figure 1-b (e.g. for NIPAAm (b), NAS ((e-(h/lactate number))/4), PLA/HEMA (h/lactate number), and OEGMA (n/(4×8.5)). In addition,

the molecular weights of copolymers were measured using gel permeation chromatography. For each composition, at least three syntheses were conducted, and the variance between feed ratios and the copolymer final compositions of copolymers was statistically analyzed using ANOVA test. Copolymer compositions were found to be consistent ($p>0.05$) with the feed ratios, as reported in Table 1 (i.e. there was no significant variance between feed ratios and the final composition of copolymers from ^{1}HNMR spectra).

Gas chromatography was used to measure the residues of different solvents which were used for the synthesis and purification of PNPHO copolymers. These organic solvents include ethyl acetate, dimethylformamide, dichloromethane, tetrahydrofuran, and diethyl ether. The concentrations of all organic solvents in the final products were below 1 ppm, demonstrating that the multiple step purification process was efficient for removing the residues of these solvents; thus it is safe for *in vitro* and *in vivo* applications.

2.2 Solubility of copolymer in PBS

One of the critical factors in synthesis of the copolymer was its solubility in water. PNPHO was comprised of a hydrophobic segment (PLA) and hydrophilic components (NAS and HEMA). We found that the concentration of PLA/HEMA, OEGMA and the lactate number in PNPHO had a significant impact on the solubility of the copolymer in PBS at 4 °C. For instance, copolymers synthesized with an OEGMA content of less than 3 mol% were insoluble in PBS. Table 1 shows that the solubility of the copolymer in PBS increased when the OEGMA content was raised from 3 mol% to 8 mol% ($p<0.001$). Increasing the hydrophobic PLA/HEMA content in the copolymer from 6 to 8 or 11 mol% decreased its solubility in PBS by 30% and 50 %, respectively. However, increasing the lactate number from 3 to 6 in the PLA/HEMA backbone had no significant impact ($p>0.05$) on the solubility of the copolymer in PBS. This result was in agreement with previous studies showing that the hydrophobicity of side chains in NIPAAm base copolymer, such as PLA, have minimal impact on the hydrophilicity of copolymers [23,24]. Therefore, by changing the lactate number, other characteristics of the copolymer such as gelling behavior and mechanical properties can be conveniently tuned with minimum impact on the solubility of copolymer in an aqueous media. Solutions of 150 mg/ml PNPHO in PBS were easily passed through an 18 G needle at room temperature, and thus this concentration of copolymer was used for further analysis. Higher concentrations of polymers could be used for other biomedical applications such as scaffold fabrication for *in vitro* cell culture.

2.3 Chemical conjugation of elastin with PNPHO and gelation mechanism

We examined the capacity of PNPHO to chemically bond with extracellular matrix proteins with primary amine groups such as elastin and collagen. In this study, α-elastin was used as this protein is soluble in buffer solutions and the hydrogels fabricated from elastin have exhibited great potential for regeneration of different tissues [11–15]. In each run, 30 mg elastin and 150 mg of PNPHO copolymer were added to one ml of PBS and gently mixed at 4 °C for 6 hr. Results for $PNPHO_{6(6)8}$ are reported here as an illustration, as this study was repeated for different compositions of PNPHO. Elastin and PNPHO were covalently bonded at pH 7.4, forming elastin-*co*-PNPHO solution.

The structure of PNPHO copolymer consisted of hydrophilic amide bonds and hydrophobic isopropyl groups. Increasing the temperature of the solution from 4 °C to 37 °C induced the dehydration of hydrophobic isopropyl groups [25] and subsequent precipitation of the conjugate system (elastin-*co*-PNPHO). Strong hydrogen bonding between water and both elastin and PNPHO traps water within the structure, resulting in the formation of a hydrogel at 37 °C. The transition from the liquid phase with low viscosity to a hydrogel upon the increase of temperature from 4 °C to 37 °C is shown in Figure 2-a. Quantitative and qualitative analyses including protein assay and structural stability analysis and ATR-FTIR spectroscopy techniques were used to confirm the covalent bonding between elastin and PNPHO.

2.3.1 Protein retention and physical stability—The stability of the hydrogels was assessed in a simulated physiological environment. In the absence of elastin, the copolymer precipitated at 37 °C, and random entanglement of polymer chains resulted in the formation of fragile and unstable hydrogel with poor physical integrity. For instance, PNPHO hydrogels underwent bulk degradation in PBS at 37 °C after 4 days as shown in Figure 2-b. In contrast, conjugation of copolymer with elastin led to the formation of covalent bonds that retained the integrity of the elastin-*co*-PNPHO hydrogel. The chemical conjugation, therefore, enhanced the stability of this elastin-containing hydrogel.

Bradford protein assay was used to assess the capacity of PNPHO that chemically bond with elastin. In the absence of the protein reactive segment (NAS) from the backbone of poly(NIPAAm-*co*-PLA/HEMA-*co*-OEGMA), a composite structure of elastin and the copolymer was formed upon the increase of temperature from 25 °C to 37 °C due to condensation of NIPAAm-*co*-PLA/HEMA-*co*-OEGMA and the coacervation of elastin at 37 °C and pH 7.4. The protein assay showed that at 37 °C more than 50 wt% and 70 wt% of elastin leached out from the structure of the hydrogel after 24 hr and 48 hr of incubation in PBS, respectively. In contrast, when NAS was present in the backbone of PNPHO, only 23 wt% of elastin released from the elastin-*co*-PNPHO hydrogels after 48 hr of washing in PBS. This result pointed to the formation of covalent bonding between elastin and the copolymer within the hydrogel structure.

2.3.2 ATR-FTIR analysis—ATR-FTIR was used to confirm the formation of covalent bonds between elastin and PNPHO in elastin-*co*-PNPHO hydrogels. Earlier studies on k-elastin and bovine elastin [26], human elastin [27], elastin-like poly(peptides) [28], synthetic elastin hydrogels [29], and α-elastin [13,30] showed typical protein peaks in amide II region (1500 cm^{-1} to 1600 cm^{-1}). The similar bands were observed for elastin in this study at 1535 cm^{-1} as shown in Figure 2-c. PNIPAAm in PNPHO also exhibited a similar band at 1535 cm^{-1}, corresponding to N-H stretching [18]. The ATR-FTIR spectra of the elastin-*co*-PNPHO hydrogel exhibited a significant shift at this region from 1535 cm^{-1} to 1545 cm^{-1}. This shift confirms a molecular interaction between elastin and PNPHO. In addition, other elastin peaks in the hydrogel spectra verify the presence of elastin in the molecular structure of elastin-*co*-PNPHO constructs. For instance, bands between 1600 cm^{-1} and 1640 cm^{-1}, contributed to β-sheet [31,32], were presented in the ATR-FTIR spectra of the elastin-*co*-PNPHO hydrogels, as shown in Figure 2-c. The presence of these β-sheet bands confirmed

intermolecular interaction and the presence of a stable protein structure [33] in elastin-*co*-PNPHO hydrogels. Earlier studies on copolymers with succinimide ester groups identify three peaks at 1740 cm^{-1}, 1763 cm^{-1}, and 1795 cm^{-1} [7,18], similar to the spectra of PNPHO in Figure 2-c. The absence or decrease in the intensity of these three bands in our elastin-*co*-PNPHO hydrogels confirmed that the succinimide ester groups of PNPHO copolymers were completely or partially engaged with amine groups of elastin. The physicochemical characteristics of elastin-*co*-PNPHO precursor hydrogels formed with different compositions of copolymer were measured to select those PNPHO compositions suitable for downstream biomedical applications. These important characterizations are gelling behavior, chemical conjugation efficiency of elastin and copolymer, degradation rate, mechanical properties and *in vitro* cell studies to assess the cytocompatibility and cell encapsulation capacity of these thermoresponsive hydrogels.

2.4 Gelling Behavior

The gelling time and temperature of injectable hydrogels are of importance to fulfill the clinical requirements. In the treatment of defects in deep tissues, gelation time of nearly 10 min is required to reach and fill the defected site with hydrogels thoroughly [34]. The gelling behavior of thermoresponsive copolymers is affected by a balance of their hydrophobicity and hydrophilicity, and their molecular weight [18,35]. At temperatures above the LCST of the copolymer, the hydrophobic backbone influences the dehydration rate of the copolymer during the condensation phase [36,37]. After condensation, the hydrophilic content of the thermoresponsive polymer allows for the formation of hydrogen bonds with water and the subsequent hydrogel formation [25,37]. Polymers with less complex molecular structures and lower molecular weights display faster dehydration rates and therefore rapid gelation [38]. In our study, the effects of lactate number (3 or 6 LA to HEMA molar ratio in PLA/HEMA), OEGMA and PLA/HEMA contents on the gelation behavior of elastin-*co*-PNPHO solutions were assessed. The gelling temperature and time taken for hydrogel formation were measured using different compositions of PNPHO.

2.4.1 Gelling Temperature—The rheological properties of elastin-*co*-PNPHO hydrogel precursors were assessed within the temperature range of 10 °C to 37 °C at an increased rate of 0.3 °C/min. Elastin was conjugated with different compositions of PNPHO and the rheological behavior of these elastin-*co*-PNPHO hydrogels were studied. The rheological behavior of three compositions of copolymers is shown as representative examples in Figures 3-a and -b. Below the LCST, all three elastin-*co*-PNPHO solutions were maintained in the liquid phase. Increasing the temperature above the LCST triggered the dehydration phase, followed by hydrogel formation.

The gelling temperature was recorded at the crossover point of dynamic storage (G′) and loss modulus (G″), as shown in Figure 3-a. After this point, the elastic response of hydrogels dominated the viscous response and the structure of the hydrogel continued to evolve as G′ increased. Throughout the analysis, the G″ remained constant at approximately 1 Pa. Figures 3-a and -b show that most of the examined elastin-*co*-PNPHO solutions formed hydrogels below 37°C. However, the LCST for elastin-*co*-$PNPHO_{6(3)8}$ was approximately 40 °C, which is above body temperature. Therefore, this composition of the copolymer was deemed

to be an unfavorable candidate for biomedical applications. The LCST above body temperature for elastin-*co*-PNPHO$_{6(3)8}$ was attributed to its high hydrophilic to hydrophobic content ratio. On the other hand, the highly hydrophobic nature of elastin-*co*-PNPHO$_{11(3)3}$ and elastin-*co*-PNPHO$_{11(6)3}$ inhibited biopolymer rehydration after the condensation phase, which led to the precipitation of conjugated polymer into a powder form with no structural integrity.

The effects of lactate number, OEGMA and PLA/HEMA molar ratio on the gelling temperature of different elastin-*co*-PNPHO solutions are presented in Figures 3-c and -e. These data show that within the range examined the lactate molar ratio in PLA/HEMA macromonomer had no significant impact ($p>0.05$) on the gelling temperature. A similar trend was observed for the effect of this parameter on the solubility of copolymer in PBS as presented in Table 1. This result suggests that the hydrophobic properties of this side-chains had no significant effect on the hydrophilic properties of PNPHO copolymer within the range examined. In contrast, the OEGMA hydrophilic backbone played a crucial role in the gelation behavior of conjugated solutions. For example, the gelling temperature of elastin-*co*-PNPHO solutions was elevated from 17 ± 2 °C to 24 ± 1 °C and 27 ± 3 °C when the OEGMA content was increased from 3 mol% (elastin-*co*-PNPHO $_{8(6)3}$) to 5 mol% (elastin-*co*-PNPHO $_{8(6)5}$) or 8 mol% (elastin-*co*-PNPHO$_{8(6)8}$), respectively ($p<0.01$). The effect of PLA/HEMA concentration as a hydrophobic segment on the gelling temperature of the copolymer was also studied. Increasing the PLA/HEMA content from 6 mol% to 8 mol% and 11 mol% significantly ($p<0.001$) decreased the gelling temperature of conjugated copolymer by approximately 20 % and 30 %, respectively. These results demonstrate that the gelling temperature of conjugated protein-PNPHO constructs can be tuned within the range of 11°C to 40 °C by adjusting their hydrophobic and hydrophilic content.

2.4.2 Gelling Time—A clinically relevant gelation time is required for injectable formulations based on their downstream application. However, excessively rapid and premature gelation may lead to needle blockage or an increase in the viscosity of the injectable solution. Both of these issues result in an ineffective administration of formulation [39]. A gelling time within the range of 5 to 9 min is recommended as optimal for clinical operations [34]. The composition of copolymers affects the gelling time of hydrogels whereby: (a) a high hydrophobic content increases the rate of condensation which leads to faster hydrogel formation and (b) increasing the molecular weight of a copolymer elevates the space impedance in polymer networks, and thus reduces the rate of hydrogel formation.

The rheological behavior of conjugated solutions at 37 °C was assessed to determine the gelling times of elastin-*co*-PNPHO solutions. The time to gelation at 37 °C was recorded as the crossover point of dynamic storage (G') and loss modulus (G''). The rheological behavior of three compositions of copolymers at 37 °C is shown by way of example in Figure 3-b. The gelling time of elastin-*co*-PNPHO solution was altered by changing its lactate number, PLA/HEMA and OEGMA content, as shown in Figure 3-d and f.

Increasing the lactate number from 3 to 6 significantly ($p<0.05$) decreased the gelling time of the conjugated system by approximately 10 %. This effect was attributed to higher hydrophobic content of copolymers with lactate number of 6 compared to 3. By raising the

PLA/HEMA content from 6 mol% to 8 mol% or 11 mol%, the gelling time was reduced 20 % and 40 %, respectively. These reductions in gelling time were attributed to increase in the hydrophobic fraction of PNPHO, which accelerates the dehydration phase of the copolymer. Lü *et al.* observed similar behavior for carboxymethylcellulose g-PNIPAAm where an increased gelation rate was attributed to an elevated hydrophobic fraction [40]. Increasing the OEGMA content from 3 mol% to 5 mol% or 8 mol% resulted in a significant ($p<0.001$) increase in gelation time from two- to three-fold, respectively. Increasing the OEGMA content of the copolymer led to steric hindrance of hydrophobic interactions during the condensation phase and thus hydrogel formation. On this basis, the rheological behavior of $PNPHO_{8(6)3}$, $PNPHO_{8(6)5}$, and $PNPHO_{8(6)8}$, shown in Figure 3-b revealed that a higher hydrophilic content means a longer gelation time.

Rheological characterization of elastin-*co*-PNPHO hydrogels at different temperatures demonstrate that it is feasible to change the gelling temperature and time of conjugated solutions by varying the composition of the copolymer. This allows us to finely tune the gelation behavior of the conjugate system based on the intended biomedical application of this class of injectable hydrogels.

2.5 Protein Retention Ratio

The incorporation of naturally derived protein in hydrogels enhances their biological activity for biomedical applications. High protein retention is an indication of structural stability and integrity of PNPHO hydrogels. Therefore, we examined the effect of composition of PNPHO on the capacity of this copolymer to conjugate with elastin. The retention ratio of elastin (fraction that is conjugated to PNPHO) within the structure of hydrogels was measured in a simulated physiological environment using a standard Bradford assay. The results in Figure 4 demonstrate the effect of lactate number, PLA/HEMA and OEGMA content on the retention of elastin within the structure of elastin-*co*-PNPHO. The retention of elastin within the elastin-*co*-PNPHO hydrogels was increased from 65 wt% to nearly 90%, by varying the composition of PNPHO copolymers. The retention of elastin within the structure of elastin-*co*-PNPHO hydrogels was promoted when nearly equimolar ratios of hydrophilic to hydrophobic segments were used in PNPHO. For instance, the elastin retention in elastin-*co*-PNPHO hydrogel after 24 hr of washing approached 91 ± 1wt% for elastin-*co*-$PNPHO_{8(6)8}$. Based on these results, four copolymer compositions with above 80% elastin retention ratio were selected for further characterizations, such as biodegradation studies and *in vitro* cell encapsulation. These copolymers included $PNPHO_{11(3)5}$, $PNPHO_{11(3)8}$, $PHPHO_{8(6)5}$, and $PNPHO_{8(6)8}$.

2.6 Bioresorbable behavior of protein-PNPHO hydrogels

Biodegradable or bioabsorbable polymers are favorable for biomedical applications. In PNPHO a degradable hydrophobic segment (PLA/HEMA) and a relatively stable hydrophilic backbone (OEGMA) were used. We hypothesized that the gradual hydrolysis of the PLA/HEMA fraction of PNPHO in a biological environment would increase the LCST of the hydrogel to above 37 °C due to a decrease in the hydrophobic content of the copolymer. This effect leads to a gradual dissolution and thus bioresorption of elastin-*co*-PNPHO hydrogels. To assess this theory, an accelerated degradation protocol was developed

in which PNPHO was immersed in a 1 M NaOH solution for a period of three days at 4 °C to degrade the PLA. After this period, the suspension was neutralized with 0.1 M HCl solution and subsequently lyophilized at −80 °C to form a white powder. ^{1}HNMR analysis of the material did not detect the characteristic peak of PLA at 5.1 ppm confirming that the PLA segment of the PNPHO copolymer was degraded. The gelling temperature of this degraded material was subsequently compared to the gelling temperature of the copolymer prior to degradation. The results depicted in Figure 5-a demonstrates a shift of gelling temperature to above 37 °C for elastin-*co*-PNPHO hydrogels that were fabricated using degraded PNPHO. For example, the gelling temperature of elastin-PNPHO$_{11(3)8}$ after accelerated degradation was significantly increased from 20.1 ± 1.0 °C to 42.2 ± 3.1 °C (p<0.001). These results confirm that the degradation of PLA in the copolymer PNPHO increases the LCST of the elastin-*co*-PNPHO to above 37 °C, which enable bioresorption of the hydrogel. The rate of bioresorption and cytocompatibility of the degradation products are important factors in defining their desirable biomedical applications. In this study, therefore, the cytocompatibility of the degradation products along with the rate of bioresorption of this class of hydrogels was investigated.

2.6.1 Cytocompatibility of elastin-co-PNPHO degradation products—The cytocompatibility of degradation products of elastin-*co*-PNPHO hydrogels was assessed. For this analysis, the degradation solution of elastin-*co*-PNPHO $_{8(6)5}$ hydrogels was added to standard culture media and then incubated with human dermal fibroblasts. At various time intervals, cell viability was measured using the MTT assay. Figure 5-b shows that the degraded material had no significant (p>0.05) influence on fibroblast viability. Furthermore, a gradual increase in cell number from day 1 to day 4 of culture (p<0.05) confirmed cytocompatibility of the degradation products.

2.6.2 Bioresorption rate of elastin-co-PNPHO hydrogels under physiological conditions—Elastin-*co*-PNPHO hydrogels with high protein retention (elastin-*co*-PNPHO $_{11(3)5}$, -PNPHO $_{11(3)8}$, -PNPHO $_{8(6)5}$, and –PNPHO$_{8(6)8}$) exhibited significantly (p<0.001) lower bioresorption rates in PBS than elastin-*co*-PNPHO$_{8(6)3}$ with a protein retention of 60%, as shown in Figure 5-c. Low bioresorption rates of elastin-*co*-PNPHO hydrogels with high elastin content were likely due to the presence of strong covalent amide bonds between elastin and PNPHO. Previous studies also showed the fast degradation rate of composite structures, generated with non-specific interactions between proteins and copolymers [41,42]. These elastin-*co*-PNPHO hydrogels with high elastin retention exhibited relatively low (< 15 %) mass loss over 30 days incubation in PBS.

Elastin-*co*-PNPHO hydrogels displayed significantly higher physical stability compared to previous injectable hydrogels fabricated with natural biopolymers. For instance, Guan *et al.* reported ~90% mass loss in thermoresponsive collagen/ NIPAAm-*co*-AAc-*co*-NAS-*co*-PLA/HEMA) hydrogel after 21 days of incubation in PBS [7]. In our study, the stability of elastin-*co*-PNPHO hydrogels was due to the covalent bonding between elastin and PNPHO. An improved physical stability of constructs was only approached in previous studies through the use of purely synthetic polymers with the commensurate risk of limited biological activity. The stability of elastin-*co*-PNPHO hydrogels under physiological

conditions is higher than synthetic based injectable hydrogels such as poly(NIPAAm-co-HEMA-co-methacrylate-polylactide (MAPLA)) that exhibit ~75% mass retention after 30 days of incubation in PBS at 37 °C [18]. The presence of natural protein in the elastin-*co*-PNPHO hydrogels might confer additional biological benefits and enhance the biological properties of the final product.

2.7 Mechanical Properties

The compressive performance of these thermoresponsive hydrogels was evaluated by conjugating elastin with $PNPHO_{11(3)5}$, $PNPHO_{11(3)8}$, $PNPHO_{8(6)5}$, and $PNPHO_{8(6)8}$. These copolymer compositions were selected because they showed the highest elastin retention and physical stability in simulated physiological environment. The compression moduli of these constructs were derived from the linear strain range of 10 to 20% shown in Figure 6-a.

The conjugation of elastin with different compositions of copolymer increased ($p<0.001$) the mechanical strength approximately two-fold compared to PNPHO hydrogels as shown in Figure 6-b. For example, elastin-*co*-$PNPHO_{11(3)5}$ has a compression modulus of 78 ± 14 kPa whereas the compression modulus of $PNPHO_{11(3)5}$ is 31 ± 4 kPa. In elastin-*co*-PNPHO hydrogels, increasing the lactate number from 3 to 6 in PLA/HEMA substantially increased the compression modulus. Changing the PLA/HEMA content had the negligible effect on the compression modulus. For instance, the compression modulus of elastin-*co*-$PNPHO_{8(6)5}$ was nearly 150 kPa, which was two-fold higher than elastin-*co*-$PNPHO_{11(3)5}$. Increasing the concentration of OEGMA from 5 mol% to 8 mol% resulted in lowering the modulus of elasticity. However, the lactate number and incorporation of elastin were the dominant factor in the mechanical strength of constructs. We found that the mechanical properties of these elastin based hydrogels can be tuned in the range of 40 kPa to 150 kPa by changing the PNPHO copolymer composition. The compression moduli in this study were in the acceptable range for some load-bearing tissues. For instance, the confined compression modulus for articular cartilage ranges from 80 kPa to 2.1 MPa [43] moving from the superficial to deep layers.

2.8 *Cell* encapsulation

After formation of cell laden elastin-*co*-PNPHO and PNPHO hydrogels at 37 °C in 15 min, the hydrogels were washed with 5 ml fresh media to remove all non-encapsulated cells. The hydrogels were then liquefied in 5 ml fresh culture media at 4 °C in 2 hr. The total number of cells and live cells in both the washing media (non-encapsulated) and encapsulated within the hydrogel were counted from flow cytometry dot-plot in Figure 7-a. The data in Figure 7-b allowed for calculations of the encapsulation efficiency of the hydrogels. Moreover, we calculated the cell viability in the elastin-*co*-PNPHO hydrogels by comparing the number of cells in the washing media and the number of cells contained within the hydrogels, as shown in Figure 7-c. These results showed that more than 85 % of cells were encapsulated within the structure of elastin-*co*-PNPHO hydrogels and immediately after encapsulation in elastin-*co*-PNPHO hydrogels the cell viability was above 80%. These results confirmed that the thermoresponsive crosslinking reaction of PNPHO copolymers is cell compatible and thus further confirmed the high potential of elastin-*co*-PNPHO hydrogels for cell encapsulation applications.

Cell-laden hydrogels were cultured *in vitro* for up to 5 days at 37 °C. At different time intervals, they were removed and liquified in fresh culture media at 4 °C within 2 hr. Figure 7-e shows the total number of live cells present within either the PNPHO copolymer or elastin-*co*-PNPHO. The numbers of live cells within both hydrogels increased significantly ($p < 0.05$) from day 1 to day 5. The ability of fibroblasts to proliferate within the structure of hydrogels was attributed to the swelling behavior of the material which allowed for the diffusion and transfer of nutrients and oxygen into the 3D structure. Fibroblast cell nuclei were stained with Hoechst 33258 at different time points up to 4 days and show that the relative numbers of encapsulated cells within elastin-*co*-PNPHO hydrogels increased significantly ($p<0.05$) over time. The classical ovoid shape of the nuclei of encapsulated fibroblast cells in Figure 7-f to -g shows that elastin-*co*-PNPHO hydrogels provided a favorable environment for cell growth and proliferation [44]. These results confirmed the cytocompatibility and favorable biological properties of elastin-*co*-PNPHO hydrogels and further justified the fabrication of these thermoresponsive hydrogels for various biomedical applications.

3 Conclusions

In this study, a new class of thermoresponsive hydrogels was developed by chemical conjugation of synthesized poly(NIPAAm-*co*-(PLA/HEMA)-*co*-OEGMA-*co*-NAS) and elastin to address the issues of low mechanical strength and inherent structural instability of currently developed injectable hydrogels. The degradation rate, mechanical and gelation properties of these injectable hydrogels are finely tunable by changing the composition of the copolymer to meet the specific biomechanical and functional requirements for different biomedical applications. These injectable and thermoresponsive hydrogels are cytocompatible and support the growth of encapsulated dermal fibroblast cells within their structure for more than 5 days. Our results demonstrate the potential of these injectable hydrogels for localized and sustained delivery of cells, and conceivably for active compounds such as antimicrobial, anti-inflammatory, growth factors and genes in a minimally invasive manner.

Acknowledgments

A.F. acknowledges the financial support from Australian Government for an Australian Postgraduate Research Award scholarship; F.D. and A.S.W. acknowledge financial support from Australian Research Council. A.S.W., the Scientific Founder of Elastagen Pty Ltd, acknowledges the financial support from Australian Defense Health Foundation, National Health and Medical Research Council and NIH EB014283.

References

1. Anseth KS, Shastri VR, Langer R. Photopolymerizable degradable polyanhydrides with osteocompatibility. Nat Biotechnol. 1999; 17:156–9. [PubMed: 10052351]
2. Choi NW, Cabodi M, Held B, Gleghorn JP, Bonassar LJ, Stroock AD. Microfluidic scaffolds for tissue engineering. Nat Mater. 2007; 6:908–15. [PubMed: 17906630]
3. Hu J, Chen B, Guo F, Du J, Gu P, Lin X, et al. Injectable silk fibroin/polyurethane composite hydrogel for nucleus pulposus replacement. J Mater Sci Mater Med. 2012; 23:711–22. [PubMed: 22231270]

4. Hoemann CD, Sun J, Légaré a, McKee MD, Buschmann MD. Tissue engineering of cartilage using an injectable and adhesive chitosan-based cell-delivery vehicle. Osteoarthritis Cartilage. 2005; 13:318–29. [PubMed: 15780645]
5. Hafemann B, Ensslen S, Erdmann C, Niedballa R, Zühlke a, Ghofrani K, et al. Use of a collagen/elastin-membrane for the tissue engineering of dermis. Burns. 1999; 25:373–84. [PubMed: 10439145]
6. Betre H, Liu W, Zalutsky MR, Chilkoti A, Kraus VB, Setton La. A thermally responsive biopolymer for intra-articular drug delivery. J Control Release. 2006; 115:175–82. [PubMed: 16959360]
7. Guan J, Hong Y, Ma Z, Wagner WR. Protein-reactive, thermoresponsive copolymers with high flexibility and biodegradability. Biomacromolecules. 2008; 9:1283–92. [PubMed: 18324775]
8. Amiram M, Luginbuhl KM, Li X, Feinglos MN, Chilkoti a. A depot-forming glucagon-like peptide-1 fusion protein reduces blood glucose for five days with a single injection. J Control Release. 2013; 172:144–51. [PubMed: 23928357]
9. Lim DW, Nettles DL, Setton La, Chilkoti A. Rapid cross-linking of elastin-like polypeptides with (hydroxymethyl)phosphines in aqueous solution. Biomacromolecules. 2007; 8:1463–70. [PubMed: 17411091]
10. Kulshrestha, AS.; Laredo, WR.; Matalenas, T.; Cooper, KL.; Technologies, A.; Llc, RM. Cyclic dithiocarbonates: novel in situ polymerizing biomaterials for medical. 2010. p. 173-83.
11. Annabi N, Mithieux SM, Boughton Ea, Ruys AJ, Weiss AS, Dehghani F. Synthesis of highly porous crosslinked elastin hydrogels and their interaction with fibroblasts in vitro. Biomaterials. 2009; 30:4550–7. [PubMed: 19500832]
12. Annabi N, Mithieux SM, Weiss AS, Dehghani F. Cross-linked open-pore elastic hydrogels based on tropoelastin, elastin and high pressure CO2. Biomaterials. 2010; 31:1655–65. [PubMed: 19969349]
13. Annabi N, Fathi A, Mithieux SM, Martens P, Weiss AS, Dehghani F. The effect of elastin on chondrocyte adhesion and proliferation on poly (ε-caprolactone)/elastin composites. Biomaterials. 2011; 32:1517–25. [PubMed: 21115195]
14. Annabi N, Mithieux SM, Zorlutuna P, Camci-Unal G, Weiss AS, Khademhosseini A. Engineered cell-laden human protein-based elastomer. Biomaterials. 2013; 34:5496–505. [PubMed: 23639533]
15. Annabi N, Tsang K, Mithieux SM, Nikkhah M, Ameri A, Khademhosseini A, et al. Highly elastic micropatterned hydrogel for engineering functional cardiac tissue. Adv Funct Mater. 2013; 23:4950–9.
16. Kim S, Healy KE. Synthesis and characterization of injectable poly(N-isopropylacrylamide-co-acrylic acid) hydrogels with proteolytically degradable cross-links. Biomacromolecules. 2003; 4:1214–23. [PubMed: 12959586]
17. Niu C, Cai M, Zhang Y, Zhou X. Biosynthetic origin of the carbon skeleton of a novel anti-tumor compound, haloroquinone, from a marine-derived fungus, Halorosellinia sp. Biotechnol Lett. 2012; 34:2119–24. [PubMed: 22829290]
18. Ma Z, Nelson DM, Hong Y, Wagner WR. Thermally responsive injectable hydrogel incorporating methacrylate-polylactide for hydrolytic lability. Biomacromolecules. 2010; 11:1873–81. [PubMed: 20575552]
19. van Dijk-Wolthuls W. A new class of polymerizable dextrans with hydrolyzable groups: hydroxyethyl methacrylated dextran with and without oligolactate spacer. Polymer (Guildf). 1997; 38:6235–42.
20. Fathi A, Lee S, Zhong X, Hon N, Valtchev P, Dehghani F. Fabrication of interpenetrating polymer network to enhance the biological activity of synthetic hydrogels. Polymer (Guildf). 2013; 54:5534–42.
21. López JM, Imperial S, Valderrama R, Navarro S. An improved Bradford protein assay for collagen proteins. Clin Chim Acta. 1993; 220:91–100. [PubMed: 8287563]
22. Compton SJ, Jones CG. Mechanism of dye response and interference in the Bradford protein assay. Anal Biochem. 1985; 151:369–74. [PubMed: 4096375]

23. Lü S, Li B, Ni B, Sun Z, Liu M, Wang Q. Thermoresponsive injectable hydrogel for three-dimensional cell culture: chondroitin sulfate bioconjugated with poly(N-isopropylacrylamide) synthesized by RAFT polymerization. Soft Matter. 2011; 7:10763.
24. Sá-Lima H, Tuzlakoglu K, Mano JF, Reis RL. Thermoresponsive poly(N-isopropylacrylamide)-g-methylcellulose hydrogel as a three-dimensional extracellular matrix for cartilage-engineered applications. J Biomed Mater Res A. 2011; 98:596–603. [PubMed: 21721116]
25. Zareie H, Volga Bulmus E, Gunning a, Hoffman a, Piskin E, Morris V. Investigation of a stimuli-responsive copolymer by atomic force microscopy. Polymer (Guildf). 2000; 41:6723–7.
26. Debelle L, Alixa J, Jacob MP, Huvenne JP, Berjot M, Sombret B, et al. Bovine elastin and kappa-elastin secondary structure determination by optical spectroscopies. J Biol Chem. 1995; 270:26099–103. [PubMed: 7592811]
27. Debelle L, Alixa J, Wei SM, Jacob MP, Huvenne JP, Berjot M, et al. The secondary structure and architecture of human elastin. Eur J Biochem. 1998; 258:533–9. [PubMed: 9874220]
28. Schmidt P, Dybal J, Rodriguez-Cabello JC, Reboto V. Role of water in structural changes of poly(AVGVP) and poly(GVGVP) Studied by FTIR and Raman spectroscopy and ab initio calculations. Biomacromolecules. 2005; 6:697–706. [PubMed: 15762632]
29. Mithieux SM, Rasko JEJ, Weiss AS. Synthetic elastin hydrogels derived from massive elastic assemblies of self-organized human protein monomers. Biomaterials. 2004; 25:4921–7. [PubMed: 15109852]
30. Annabi N, Fathi A, Mithieux SM, Weiss AS, Dehghani F. Fabrication of porous PCL/elastin composite scaffolds for tissue engineering applications. J Supercrit Fluids. 2011; 59:157–67.
31. Hu X, Kaplan D, Cebe P. Determining Beta-Sheet Crystallinity in Fibrous Proteins by Thermal analysis and infrared spectroscopy. Macromolecules. 2006; 39:6161–70.
32. Hu, X.; Lu, Q.; Kaplan, DL.; Cebe, P. Microphase separation controlled -sheet crystallization kinetics in fibrous proteins. 2009. p. 2079-87.
33. Hu X, Wang X, Rnjak J, Weiss AS, Kaplan DL. Biomaterials derived from silk-tropoelastin protein systems. Biomaterials. 2010; 31:8121–31. [PubMed: 20674969]
34. Zheng Shu X, Liu Y, Palumbo FS, Luo Y, Prestwich GD. In situ crosslinkable hyaluronan hydrogels for tissue engineering. Biomaterials. 2004; 25:1339–48. [PubMed: 14643608]
35. Matsuda SOT. Poly (N-isopropylacrylamide) (PNIPAM) -grafted gelatin as thermoresponsive three-dimensional artificial extracellular matrix: molecular and formulation parameters vs. cell proliferation potential. Journal of Biomaterials Science. 2012:37–41.
36. De Las Heras Alarcon C, Pennadam S, Alexander C. Stimuli responsive polymers for biomedical applications. Chem Soc Rev. 2005; 34:276–85. [PubMed: 15726163]
37. Heskins M, Guillet JE. Solution properties of poly(N-isopropylacrylamide). J Macromol Sci Part A - Chem. 1968; 2:1441–55.
38. Yoshida R, Uchida K, Kaneko Y, Sakai K, Kikuchi A, Sakurai Y, et al. Comb-type grafted hydrogels with rapid deswelling response to temperature changes. Nature. 1995; 374:240–2.
39. He C, Kim SW, Lee DS. In situ gelling stimuli-sensitive block copolymer hydrogels for drug delivery. J Control Release. 2008; 127:189–207. [PubMed: 18321604]
40. Lü S, Liu M, Ni B. Degradable, injectable poly(N-isopropylacrylamide)-based hydrogels with low gelation concentrations for protein delivery application. Chem Eng J. 2011; 173:241–50.
41. Roberts MJ, Bentley MD, Harris JM. Chemistry for peptide and protein PEGylation. Adv Drug Deliv Rev. 2002; 54:459–76. [PubMed: 12052709]
42. PASUT G, Veronese FM. PEGylation of proteins as tailored chemistry for optimized bioconjugates. Adv Polym Sci. 2006; 192:95–134.
43. Chena C, Bae WC, Schinagl RM, Sah RL. Depth- and strain-dependent mechanical and electromechanical properties of full-thickness bovine articular cartilage in confined compression. J Biomech. 2001; 34:1–12. [PubMed: 11425068]
44. Mao X, Chu C-L, Mao Z, Wang J-J. The development and identification of constructing tissue engineered bone by seeding osteoblasts from differentiated rat marrow stromal stem cells onto three-dimensional porous nano-hydroxylapatite bone matrix in vitro. Tissue Cell. 2005; 37:349–57. [PubMed: 16002113]

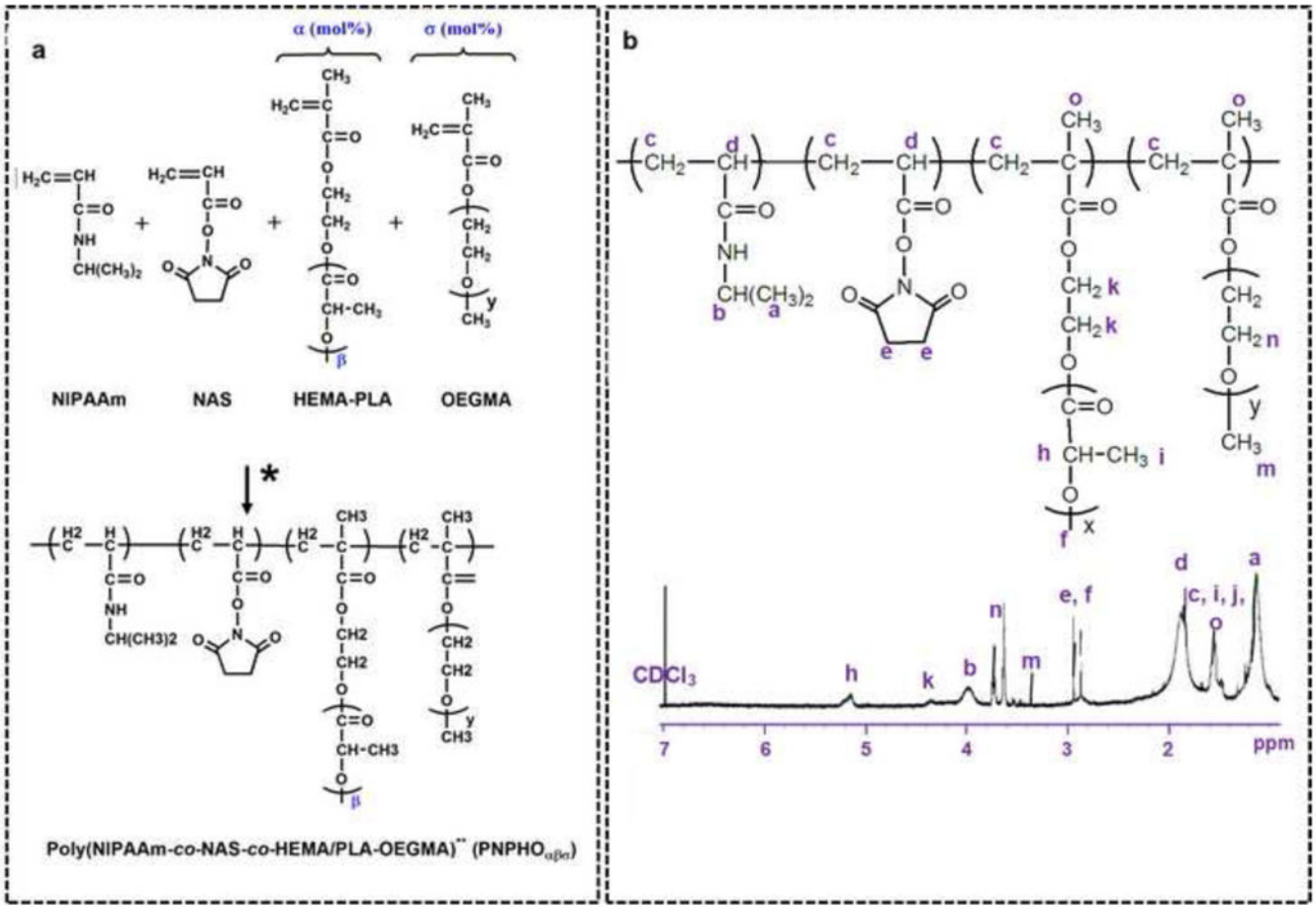

Figure 1.

The reaction scheme for the synthesis of poly(NIPAAm-*co*-NAS-*co*-PLA/HEMA-*co*-OEGMA) copolymer, denoted as PNPHOσβα (*:Synthesized in dimethylformamide at 70 °C, 24 hr, using 4, 4′-azobis 4-cyanovaleric acid (a), ^{1}HNMR spectra of PNPHO copolymer (b).

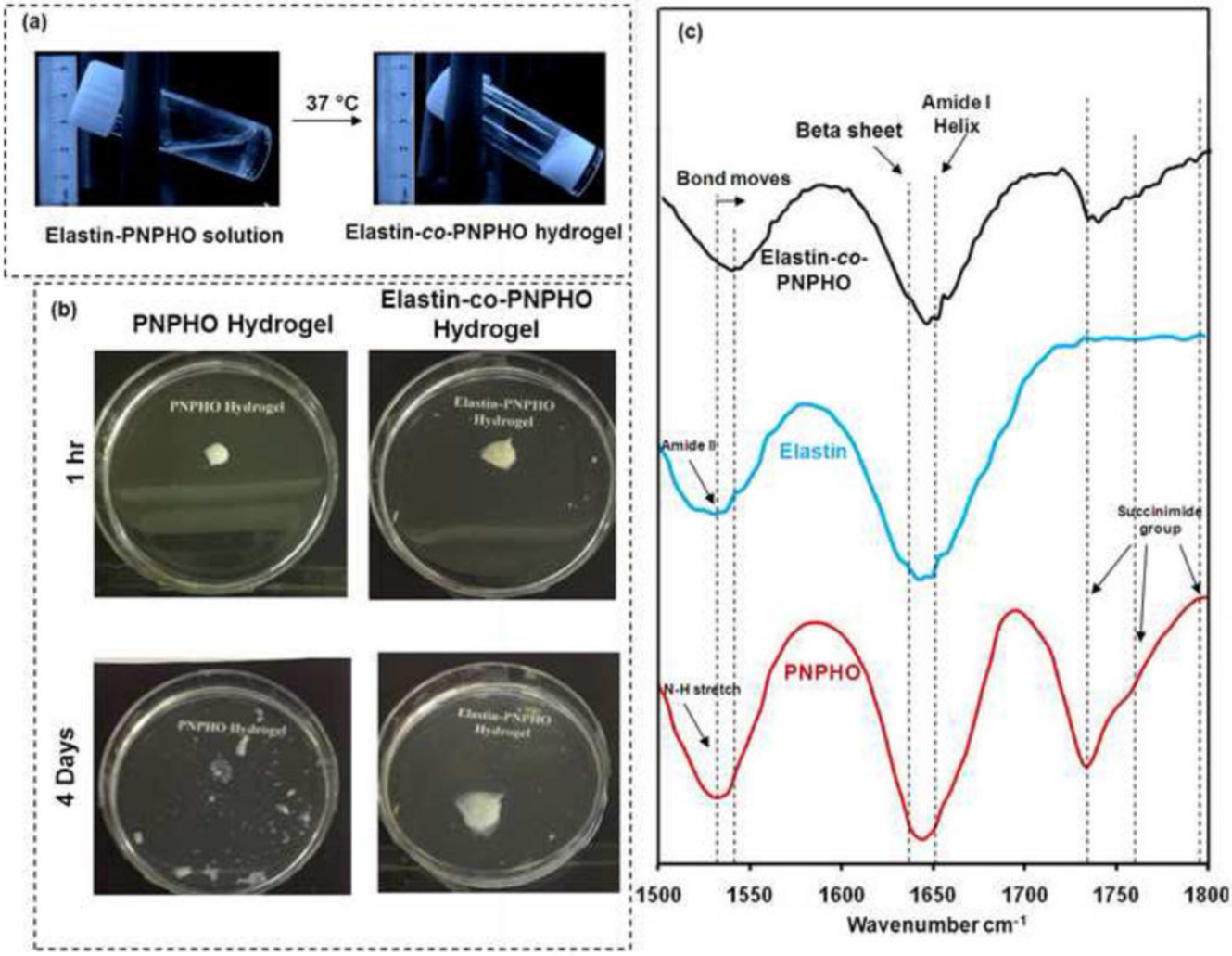

Figure 2.

Thermal-behaviour of elastin-*co*-PNPHO hydrogels at 37 °C (a), and stability test of PNPHO and elastin-co-PNPHO hydrogels in a physiological environment (b), and FTIR spectra of PNPHO copolymer, elastin and elastin-*co*-PNPHO hydrogels (c).

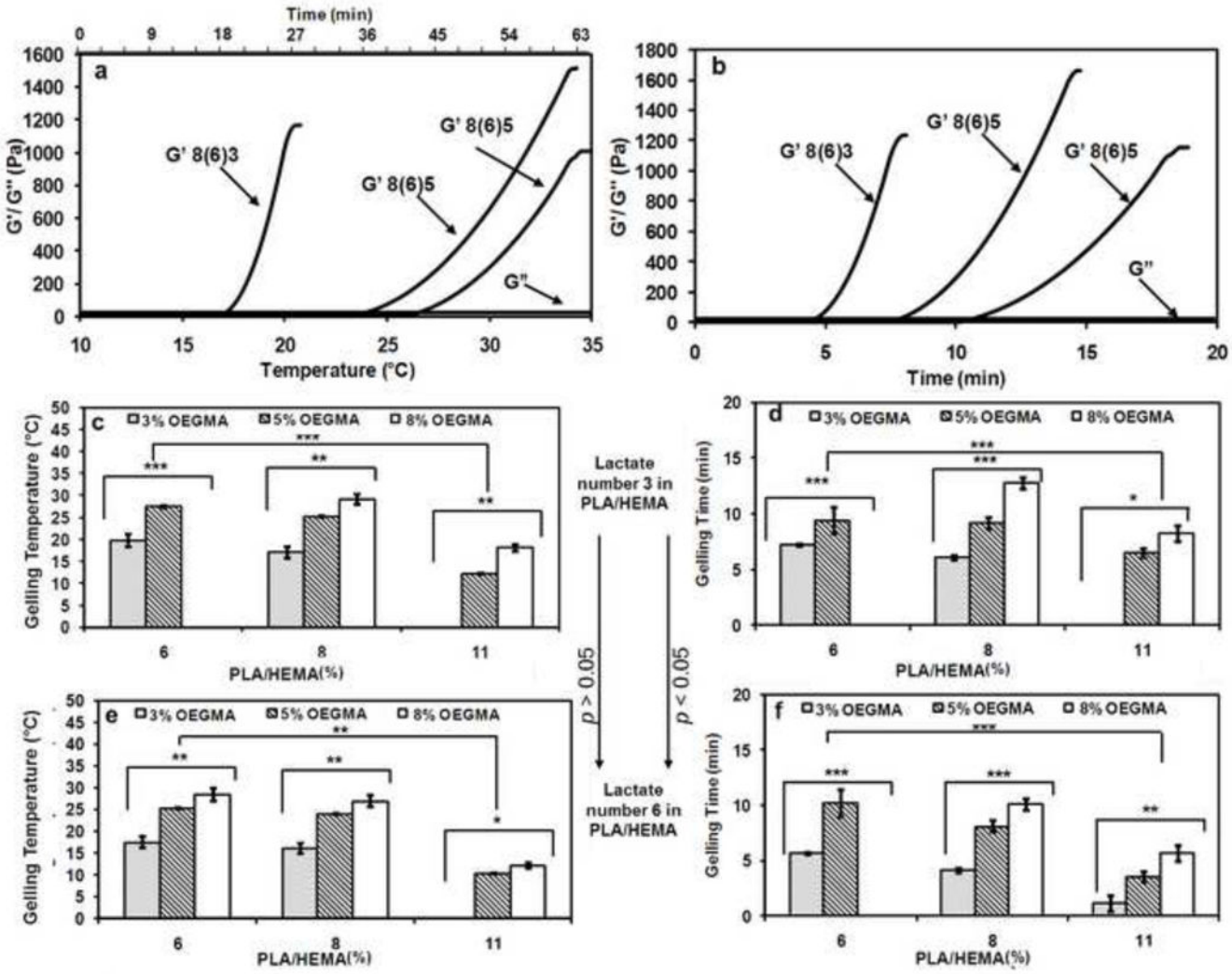

Figure 3.

Effect of temperature on rheological behavior of elastin-*co*-PNPHO hydrogels, prepared with different compositions of PNPHO copolymer (a), rheological behavior of elastin-*co*-PNPHO hydrogels at 37 °C (b) gelling temperature (c and e) and gelling time (d and f) of these hydrogels with lactate number of 3 (c and d) and 6 (e and f) in PLA/HEMA (*, **, and *** represent $p<0.05$, < 0.01, and <0.001, respectively).

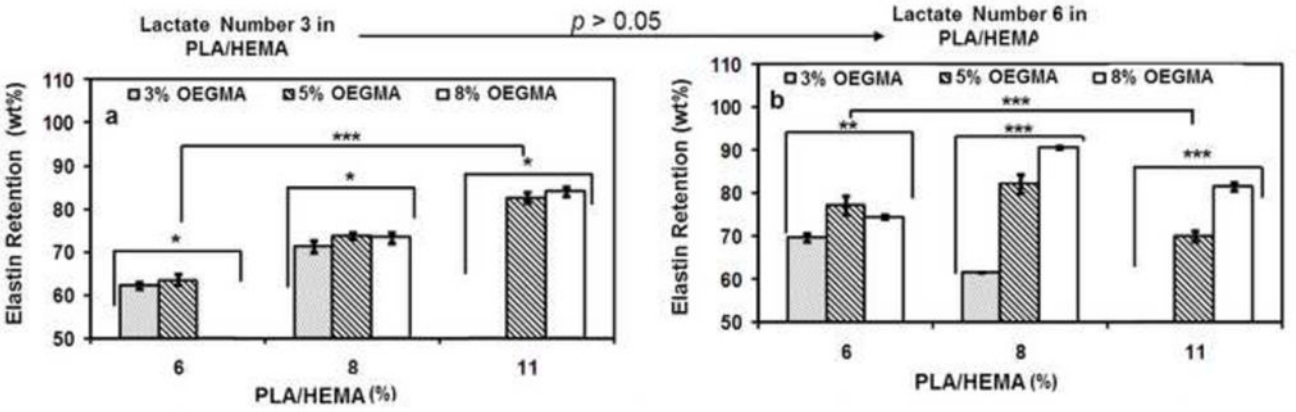

Figure 4.

Elastin retention rate in elastin-*co*-PNPHO hydrogel fabricated with different compositions of PNPHO and with lactate number of 3 (a) and 6(b) (*, **, and *** represent $p<0.05$, < 0.01, and <0.001, respectively).

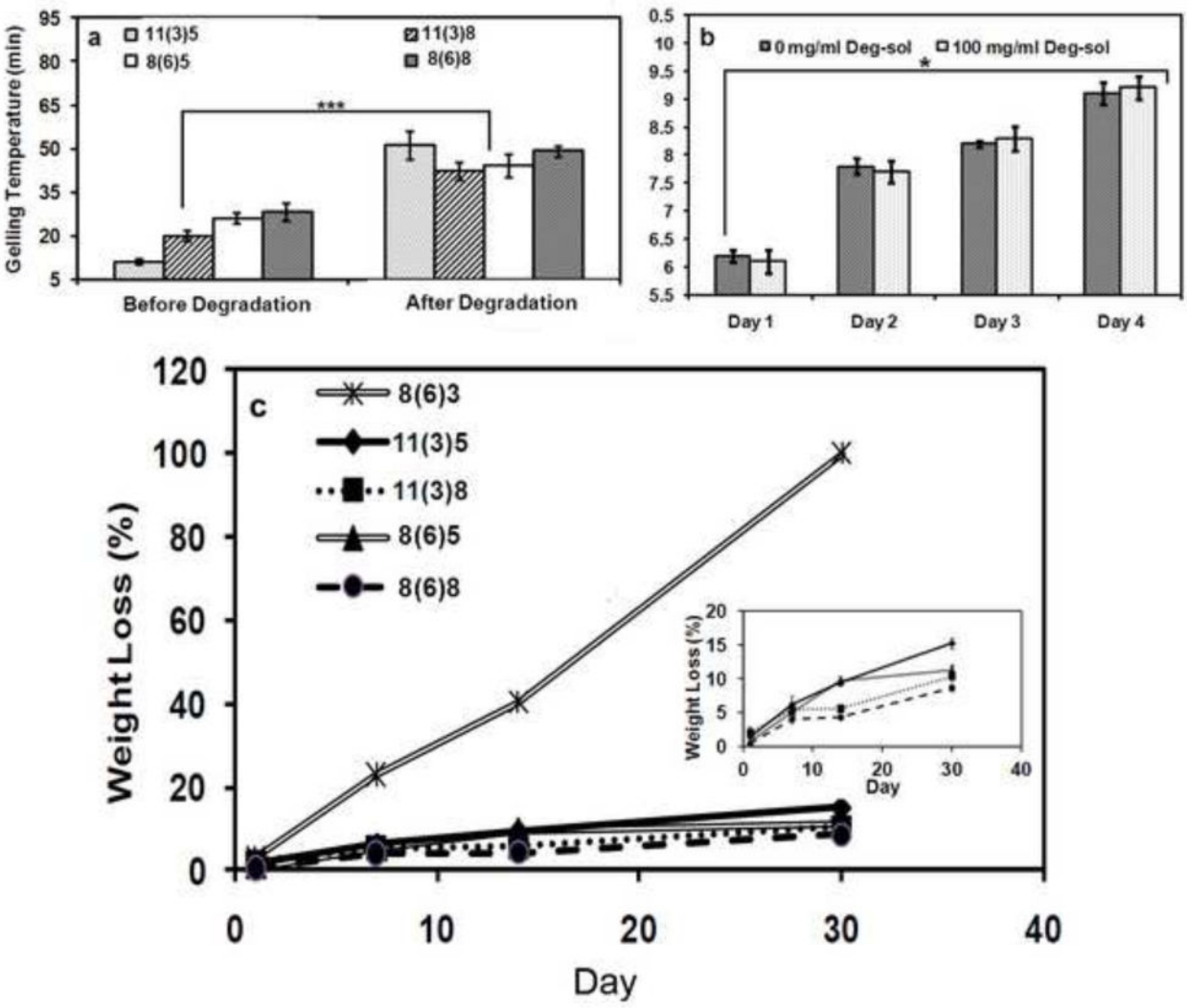

Figure 5.

Gelling temperature of hydrogel precursors formed with PNPHO copolymer before and after cleavage of PLA segment (a) and *in vitro* cytocompatibility study of degradation products by measuring the growth of dermal fibroblast in culture media with and without addition of degradation solution (b) and mass loss of different elatin-*co*-PNPHO hydrogels over time in PBS at 37 °C (c). The legend refer to different compositions of PNPHO as PLA/HEMA(lactate number)OEGMA mol%.

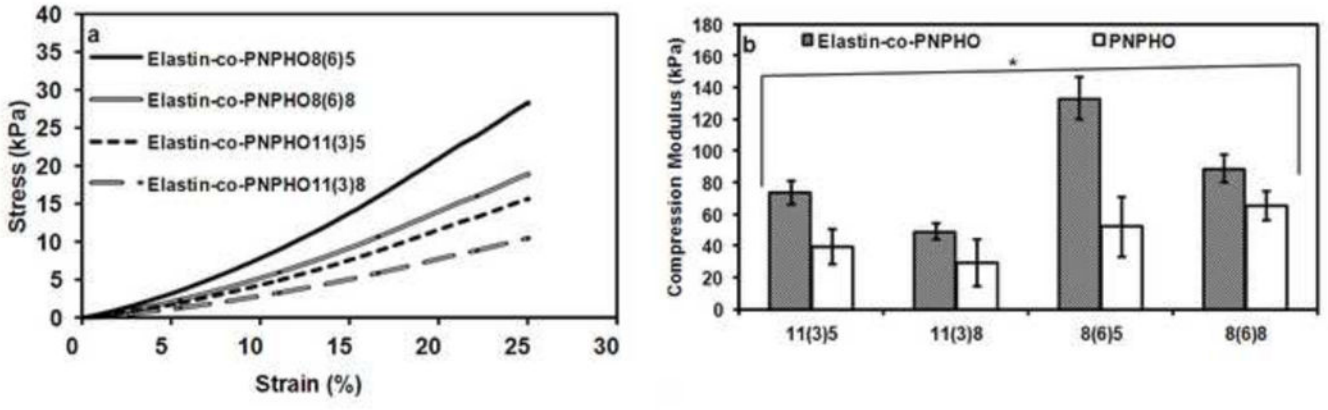

Figure 6.

Stress-strain curve of elastin-*co*-PNPHO hydrogels fabricated with different compositions of PNPHO (a) and the compression modulus of PNPHO and elastin-*co*-PNPHO hydrogels (b) (* respresents $p<0.05$).

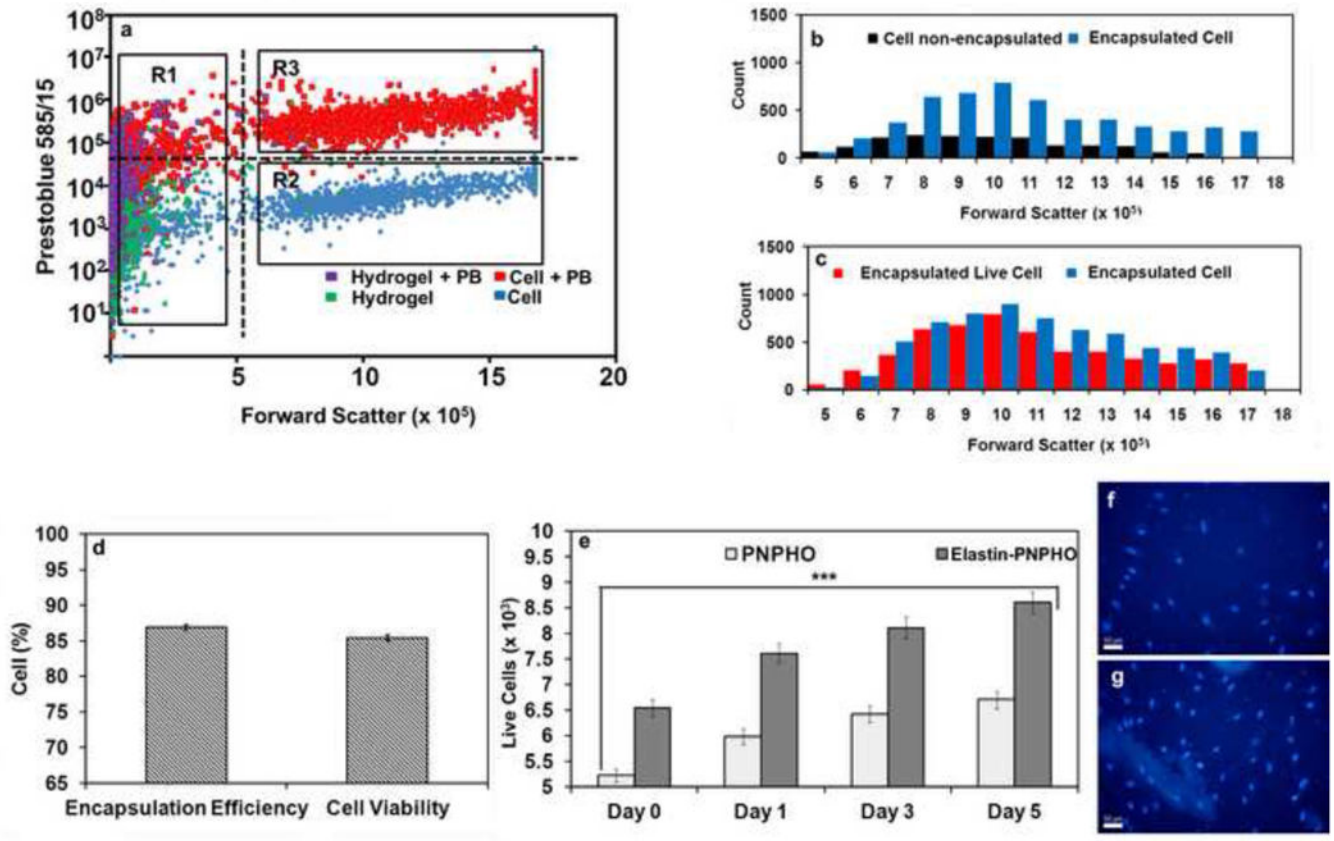

Figure 7.

Flow cytometry dot-plot of cell laden elastin-*co*-PNPHO hydrogels with Prestoblue staining, collected with 480/30 filter versus forward scatter (a), histogram of total number of cells in supernatant (non-encapsulated) and cell laden in elastin-*co*-PNPHO hydrogel (b), histogram of total number of cells and live cells, encapsulated within elastin-*co*-PNPHO hydrogels (c), encapsulation efficiency and cell viability in elastin-*co*-PNPHO hydrogels (d) cell proliferation from day 0 to day 4 in elastin-co-PNPHO hydrogels (e) and encapsulated fibroblast in elastin-*co*-PNPHO hydrogels after one day (f) and 4 days (g) of culture, nucleus stained with Hoechst 33258 dye and visualized at 350 nm and scale bar is 50 μm.

Table 1

Molar ratios of monomers used for the synthesis of PNPHO copolymer and the final composition, molecular weight (achieved from 1HNMR and gel permeation chromatography**),** and gelling temperature and time of copolymers (gelling temperature and time of copolymers are compared in Figure 3).

Monomers molar ratio[1]	Final composition of copolymer[1]	Mw	PBS Solubility (mg/ml)	Gelling Temperature (°C)	Gelling Time (min)
6(3)3/7/84	8.7(3)/3.4/7.9/80	21,212	270 ± 15	20 ± 3	7 ± 1
8(3)/3/7/82	10.9(3)/3.9/8.2/77	21,451	255 ± 5	17 ± 2	6 ± 1
11(3)/3/7/79	11(3)/3/8/78	22,444	170 ± 15	Precipitate	Precipitate
6(3)/5/7/82	7.8(6)/5/8.2/79	22,551	470 ± 20	27 ± 1	9 ± 3
8(3)/5/7/80	9.1(6)/6.5/8.4/76	23,544	360 ± 5	25 ± 1	8 ± 2
11(3)/5/7/77	9.1(6)/7/7.9/76	23,001	270 ± 10	13 ± 1	7 ± 2
6(3)/8/7/79	8.2(6)/7/7/77.8	25,541	555 ± 10	~ 40	Not Measured
8(3)/8/7/77	8.8(6)/8.1/8.1/75	25,550	410 ± 5	30 ± 2	13 ± 2
11(3)/8/7/74	11.8(6)/8/8.2/72	27,002	300 ± 5	18 ± 2	9 ± 3
6(6)/3/7/84	6.8(6)/3/8.5/81.5	23,211	260 ± 20	17 ± 2	5 ± 1
8(6)/3/7/82	9.1(6)/3/8/79.9	22,551	190 ± 10	24 ± 1	3 ± 1
11(6)/3/7/79	12.2(6)/3.2/8.6/76	24,555	165 ± 5	Precipitate	Precipitate
6(6)/5/7/82	6(6)/5.6/8.4/80	27,521	375 ± 15	26 ± 1	10 ± 3
8(6)/5/7/80	6(6)/8.1/5.5/8.4/77	25,521	360 ± 20	24 ± 1	7 ± 2
11(6)/5/7/77	11.1(6)/5.6/8/75.3	26,555	275 ± 10	10 ± 1	4 ± 1
6(6)/8/7/79	9(6)/8.5/8/74.5	28,452	550 ± 15	29 ± 3	Not gelled
8(6)/8/7/77	10(6)/9/8.3/72.6	28,881	385 ± 10	27 ± 3	11 ± 2
11(6)/8/7/74	11(6)/8/7/74	27,885	275 ± 10	12 ± 2	5 ± 2

[1]. The codes represent PLA-HEMA(lactate number)/OEGMA/NAS/NIPAAm mol%.